

# Superluminal Behaviors of Modified Bessel Beams

Z. Y. Wang <sup>\*</sup>, C. D. Xiong

*University of Electronic Science and Technology of China, Chengdu, Sichuan 610054, P.R. China*

## Abstract

Much experimental evidence of superluminal phenomena has been available by electromagnetic wave propagation experiments, with the results showing that the phase time do describe the barrier traversal time. Based on the extrapolated phase time approach and numerical methods, we show that the group velocities of modified Bessel beams can be superluminal, and obtain the following results: 1) the group velocities increase with the increase of propagation distance, which is similar to the evanescent plane-wave cases, but in detail, there has some differences between them; 2) for large wave numbers, the group velocities fall off as the wave numbers increase, which is similar to the evanescent plane-wave cases; 3) for small wave numbers, the group velocities increase with the increase of wave numbers, this is different from the evanescent plane-wave cases.

**PACS numbers:** 41.20.Jb, 42.25.Bs, 42.50.Dv

<sup>\*</sup>Electronic address: [zywang@uestc.edu.cn](mailto:zywang@uestc.edu.cn)

## 1. Introduction

As we known, for a given wave packet, there are many different ways we can expand it, e.g., we can be expand it as the superposition of the plane waves, of the cylindrical waves or of the spherical waves, etc., which depends on the choice of curvilinear coordinate systems. Nevertheless, all the physical properties of the wave packet are independent of coordinate transformations, or, not dependent on the expansion forms of the wave packet. In particular, in contrary to some literatures [1-3], an ordinary Bessel beam described by the Bessel functions of real argument, actually has not the superluminal behaviors [4-7], just as other beams such as the plane waves, etc. In fact, the claim that, in the absence of dispersion the phase and the group velocity components along a given direction (say, the  $z$ -axis direction) are equal, is wrong, provided that the totally wave number vector (say,  $\vec{k}$ ) is not parallel to the  $z$ -axis direction. That is to say, let  $k_z$  denote the projection of  $\vec{k}$  in the  $z$ -axis direction,  $\omega$  the frequency, the phase velocity component is  $v_{pz} = \omega/k_z$  while the group velocity component  $v_{gz} = d\omega/dk_z$ , one can show  $v_{pz} \neq v_{gz}$  if  $|k_z| \neq |\vec{k}|$ . It is highly important to note that, the phase velocity vector  $\vec{v}_p$  does not obey the usual vector addition: the magnitude of the phase velocity component  $v_{pz}$  is greater than that of  $\vec{v}_p$  itself if  $|k_z| \neq |\vec{k}|$ . For example, when electromagnetic waves are reflected back and forth by perfectly conducting walls as they propagate along the length of a hollow waveguide, their phase velocity components along the waveguide are greater than the speed  $c$  of light in vacuum, while the instantaneous total phase velocities are always the speed  $c$  within the waveguide. In a word, the

phase velocity has the property of geometric artifact.

However, contrary to the ordinary Bessel beam of real argument, we shall show that modified Bessel beams, described by the Bessel functions of imaginary argument, do have the superluminal behaviors.

To avoid confusion, let us point out that, the Bessel beams, via which the superluminal phenomena have been studied before [1-7], are the ones that propagate along the symmetry axis of a cylinder (that has no end plates and is open on both ends), their plane wavefront is perpendicular to the symmetry axis, while the Bessel beams studied in this paper correspond to the ones that propagate along the radial direction of a cylinder (that has no lateral face and is open on circumference), with a cylindrical wavefronts perpendicular to the radial direction.

## 2. Modified Bessel beams and evanescent waves

In Cartesian coordinate system  $(x, y, z)$ , assume that a hollow metal cylinder of radius  $\rho \rightarrow +\infty$  has its axis coincident with the  $z$ -axis, two perfectly conducting plates of radius  $\rho \rightarrow +\infty$  are  $L$  apart, they form two parallel end plates of the cylinder and are respectively located at  $z = -L/2$  and  $z = L/2$ . The cylinder has no lateral face. A linear antenna with length  $d \leq L$  is placed at the symmetry axis of the cylinder extending from  $z = -d/2$  to  $z = d/2$ , and  $d$  is small compared to the wavelength  $\lambda$  of the fields produced by the antenna. In the present case, the boundary condition suggests the use of cylindrical coordinate system  $(r, \theta, z)$  ( $x = r \cos \theta$ ,  $y = r \sin \theta$ ). Let  $\omega$  denote the angular frequency,  $k = \omega/c$  the wave number,  $c$  the velocity of light in vacuum. As we known, the fields in the far

zone  $kr \gg 1$  (where  $r$  is the distance from the source to the field point) represent the radiation fields of the antenna, for the objectives of the present paper, we limit our attention to just the far-zone fields. Let  $\varphi(r, \theta, z, t) = u(r, \theta, z) \exp(i\omega t)$  denote the radiation field intensities of the antenna, in cylindrical coordinates  $(r, \theta, z)$ , the wave equation for  $\varphi$  takes the form ( $kr \gg 1$ )

$$\frac{1}{r} \frac{\partial}{\partial r} \left( r \frac{\partial \varphi}{\partial r} \right) + \frac{1}{r^2} \frac{\partial^2 \varphi}{\partial \theta^2} + \frac{\partial^2 \varphi}{\partial z^2} - \frac{1}{c^2} \frac{\partial^2 \varphi}{\partial t^2} = 0 \quad (1)$$

Or using  $\varphi(r, \theta, z, t) = u(r, \theta, z) \exp(i\omega t)$  and  $k = \omega/c$ , one has

$$\frac{1}{r} \frac{\partial}{\partial r} \left( r \frac{\partial u}{\partial r} \right) + \frac{1}{r^2} \frac{\partial^2 u}{\partial \theta^2} + \frac{\partial^2 u}{\partial z^2} + k^2 u = 0 \quad (2)$$

In our case, the boundary conditions are

$$u|_{\theta=0} = u|_{\theta=2\pi}, \quad \frac{\partial u}{\partial \theta}|_{\theta=0} = \frac{\partial u}{\partial \theta}|_{\theta=2\pi}, \quad u|_{z=\pm L/2} = 0, \quad u|_{r=+\infty} \neq +\infty \quad (3)$$

Where the boundary condition  $u|_{r=+\infty} \neq +\infty$  is due to the fact that, the radiation fields  $\varphi(r, \theta, z, t)$  are emitted by the antenna placed at the axis of the cylinder and propagate radially from  $r = r_0 \gg 1/k$  to  $r = \rho \rightarrow +\infty$ .

Assume a separable solution  $u(r, \theta, z) = R(r)\Theta(\theta)Z(z)$ , and substitute into Equ. (2), one can obtain ( $\Theta'(\theta) \equiv \partial \Theta / \partial \theta$ )

$$\begin{cases} \frac{d^2 \Theta}{d\theta^2} + \eta \Theta = 0 \\ \Theta(0) = \Theta(2\pi), \Theta'(0) = \Theta'(2\pi) \end{cases} \quad (4)$$

$$\begin{cases} \frac{d^2 Z}{dz^2} + \alpha Z = 0 \\ Z(\pm L/2) = 0 \end{cases} \quad (5)$$

$$\begin{cases} \frac{1}{r} \frac{d}{dr} \left( r \frac{dR}{dr} \right) + (k^2 - \alpha - \frac{\eta}{r^2}) R = 0 \\ R(+\infty) \neq +\infty, 1/k \ll r_0 \leq r < +\infty \end{cases} \quad (6)$$

The eigenvalues and eigenfunctions of Equ. (4) are, respectively

$$\begin{cases} \eta_m = m^2 \\ \Theta_m(\theta) = A_m \cos m\theta + B_m \sin m\theta \end{cases}, (m = 0, 1, 2, 3, \dots) \quad (7)$$

with  $A_m$  and  $B_m$  constants. Likewise, the eigenvalues and eigenfunctions of Equ. (5) are, respectively

$$\begin{cases} \alpha_n = (2n\pi/L)^2 \\ Z_n(z) = \sin(2zn\pi/L) \end{cases}, (n = 1, 2, 3, \dots) \quad (8)$$

Then Equ. (6) becomes

$$\begin{cases} \frac{1}{r} \frac{d}{dr} (r \frac{dR}{dr}) + [k^2 - (\frac{2n\pi}{L})^2 - \frac{m^2}{r^2}] R = 0 \\ R(+\infty) \neq +\infty, 1/k \ll r_0 \leq r < +\infty \end{cases} \quad (9)$$

Let  $k_n \equiv 2n\pi/L$  and  $\sigma_n \equiv \sqrt{k^2 - k_n^2} > 0$ , the radial equation (9) can be put in a standard form by the change of variable  $s = \sigma_n r$ , i.e., the Bessel equation. In terms of the order- $m$  Bessel functions of the first and second kinds (the latter also called the order- $m$  Neumann functions), i.e.

$$J_m(x) = \sum_{l=0}^{\infty} (-1)^l \frac{1}{l! \Gamma(m+l+1)} \left(\frac{x}{2}\right)^{m+2l}, \quad Y_m(x) = \lim_{\nu \rightarrow m} \frac{J_{\nu}(x) \cos \nu \pi - J_{-\nu}(x)}{\sin \nu \pi} \quad (10)$$

where  $\Gamma(z) \equiv \int_0^{\infty} e^{-t} t^{z-1} dt$ ,  $l, \nu = 0, 1, 2, 3, \dots$ , one can write the solutions of Equ. (9) as, generally

$$R_{mn}(r) = C_m J_m(h_n r) + D_m Y_m(h_n r) \quad (11)$$

with  $C_m$  and  $D_m$  constants. Using Equs. (7)-(11), one can obtain the general solution of Equ. (1)

$$\varphi(r, \theta, z, t) = \sum_{m,n} [R_{mn}(r) \Theta_m(\theta) Z_n(z)] \exp(i\omega t) \quad (12)$$

For each given  $n = 1, 2, 3, \dots$ , let  $\lambda_c(n) \equiv 2\pi/k_n = L/n$ , we refer to  $\lambda_c(n)$  as the order- $n$  cutoff wavelength. Obviously, as  $k^2 \geq k_n^2 = (2n\pi/L)^2$  (or  $\lambda < \lambda_c(n)$ ),

the radial solution  $R(r)$  of Equ. (9) is described by the Bessel functions of real argument (i.e., the ordinary Bessel functions), and the radiation fields  $\varphi(r, \theta, z, t)$  described by the ordinary Bessel beams represent the traveling waves that propagate along the radial direction of the cylinder, with a cylindrical wavefront perpendicular to the radial direction.

On the other hand, as  $k^2 < k_n^2 = (2n\pi/L)^2$  (or  $\lambda > \lambda_c(n)$ ), the radial solution  $R(r)$  is described by the Bessel functions of imaginary argument (or the modified Bessel functions). In terms of the modified Bessel functions of the first and second kind, namely

$$I_m(x) \equiv e^{-im\pi/2} J_m(ix), \quad K_m(x) \equiv \lim_{\nu \rightarrow m} \frac{\pi}{2 \sin \nu \pi} [I_{-\nu}(x) - I_\nu(x)] \quad (13)$$

the radial solution of Equ. (9) can be written as  $R_{mn}(r) = E_m I_m(g_n r) + F_m K_m(g_n r)$ , where  $g_n \equiv \sqrt{k_n^2 - k^2} > 0$ ,  $E_m$  and  $F_m$  are constants. Seeing that  $u|_{r=+\infty} \neq +\infty$  and  $1/k \ll r_0 \leq r < +\infty$ , the coefficients  $E_m \equiv 0$ , then

$$R_{mn}(r) = F_m K_m(g_n r) \quad (14)$$

The asymptotic form  $K_m(x) \sim \sqrt{\pi/2x} \exp(-x)$  (as  $x \rightarrow +\infty$ ) implies that, in the present case, the radiation fields  $\varphi(r, \theta, z, t)$  become the evanescent fields. Therefore, as  $\lambda > \lambda_c(n)$ , the radiation fields  $\varphi(r, \theta, z, t)$  described by *the modified Bessel beams* correspond to evanescent waves.

### 3. Superluminal behaviors of modified Bessel beams

In order to study the superluminal behaviors of modified Bessel beams, let us have recourse to the analogy between the behaviors of modified Bessel beams and the quantum tunneling of particles. For this we assume that the separation  $L$  between

the two parallel end plates of the cylinder satisfies

$$L = \begin{cases} L_0 > 2\pi/k, 0 \leq r \leq r_1 \\ L_1 < 2\pi/k, r_1 \leq r \leq r_2 \\ L_0 > 2\pi/k, r_2 \leq r < +\infty \end{cases} \quad (15)$$

Where  $r_1 > r_0 \gg 1/k$  (note that what we are interested in is the far-zone fields of the antenna). Consider that the radiation fields  $\varphi(r, \theta, z, t)$  with wave numbers distributed sharply around the given  $k$  propagate along the radial direction, and because of the axial symmetry, we limit our attention to just the radial solution  $R(r)$  and the time factor  $\exp(i\omega t)$  is omitted. For simplicity, let  $m=0$  and  $n=1$  without loss of generality, then Equ. (9) becomes

$$\begin{cases} \frac{1}{r} \frac{d}{dr} (r \frac{dR}{dr}) + h^2 R = 0 & (r \gg 1/k) \\ R(+\infty) \neq +\infty \end{cases} \quad (16)$$

Where

$$h = \begin{cases} h_0 = \sqrt{k^2 - (2\pi/L_0)^2}, r_0 \leq r \leq r_1 \\ h_1 = i\sqrt{(2\pi/L_1)^2 - k^2} \equiv i\kappa, r_1 \leq r \leq r_2 \\ h_0 = \sqrt{k^2 - (2\pi/L_0)^2}, r_2 \leq r < +\infty \end{cases} \quad (17)$$

Owing to Equ. (15), one has  $h_0 > 0$  and  $\kappa > 0$ . In terms of the Hankel functions of the first and second kind

$$H_m^{(1)}(x) \equiv J_m(x) + iY_m(x), \quad H_m^{(2)}(x) \equiv J_m(x) - iY_m(x) \quad (18)$$

as well as the modified Bessel functions of the first and second kind (given by Equ. (13)), the solutions of Equ. (16) can be written as

$$R(r) = \begin{cases} R_1(r) = a_1 H_0^{(1)}(h_0 r) + a_2 H_0^{(2)}(h_0 r), r_0 \leq r < r_1 \\ R_2(r) = b_1 I_0(\kappa r) + b_2 K_0(\kappa r), r_1 \leq r < r_2 \\ R_3(r) = \eta H_0^{(1)}(h_0 r), r_2 \leq r < +\infty \end{cases} \quad (19)$$

The five unknown quantities  $a_1, a_2, b_1, b_2, \eta$ , in general, as the functions of  $k$

and  $r$ , are restricted by the equations that impose continuity of  $R(r)$  and  $dR(r)/dr$  at  $r = r_1$  and  $r = r_2$ . For the sake of simplicity, we assume that the derivatives of  $a_1$ ,  $a_2$ ,  $b_1$ ,  $b_2$  and  $\eta$  with respect to  $r$  approach zero for  $kr \gg 1$  (such that these derivatives can be omitted), this simplification is justified because the cylindrical waves approach plane waves as  $kr \rightarrow +\infty$ . In view of the fact that the Hankel functions  $H_m^{(1)}(x)$  and  $H_m^{(2)}(x)$  (multiplied by the time factor  $\exp(i\omega t)$ ) express outward- and inward-propagating cylindrical wave solutions of the cylindrical wave equation, respectively, in our case the quantity  $H_0^{(1)}(h_0 r)$  represents the incident wave propagating from  $r = r_0 \gg 1/k$  to  $r = r_1$ , while  $H_0^{(2)}(h_0 r)$  represents the reflected wave that is reflected at  $r = r_1$ . Therefore the quantity  $|a_2|^2 / |a_1|^2$  represents the reflection probability, and the transmission probability is  $|\eta|^2 / |a_1|^2$ . Likewise, the quantities  $K_0(\kappa r_2)$  and  $I_0(\kappa r_2)$  are the evanescent and anti-evanescent waves, respectively. In the present case, the annular region between  $r = r_1$  and  $r = r_2$  plays the role of photonic potential barrier.

Furthermore, let us consider that two Bessel beams  $H_0^{(1)}(-h_0 r)$  and  $H_0^{(1)}(h_0 r)$  are simultaneously produced by the antenna and  $H_0^{(1)}(-h_0 r)$  propagates in the negative direction of the  $x$ -axis, while  $H_0^{(1)}(h_0 r)$  propagates in the positive  $x$ -direction, the former is partially reflected at  $x = -r_1$  and forms  $H_0^{(2)}(-h_0 r)$ , the latter is partially reflected at  $x = r_1$  and produces  $H_0^{(2)}(h_0 r)$ , and so on (they are partially reflected back and forth within the zone  $0 < r \leq r_1$ ). Using the relation  $H_0^{(1)}(-h_0 r) = -H_0^{(2)}(h_0 r)$  etc., and choosing the appropriate quantities  $a_1$ ,  $a_2$ ,  $b_1$ ,  $b_2$ ,  $\eta$  (as the functions of  $k$  and  $r$ ), one can impose the condition  $\lim_{r \rightarrow 0} R(r) \neq \infty$ .

However, in our case, we are interested only in the radiation fields in the far zone of the antenna where  $1/k \ll r < +\infty$  and give a general expression Equ. (19) for  $1/k \ll r < +\infty$ .

Now let us apply the continuity of  $R(r)$  and  $dR(r)/dr$  at  $r = r_1$  and  $r = r_2$ , and  $dH_0^{(1)}(x)/dx = -H_1^{(1)}(x)$ ,  $dH_0^{(2)}(x)/dx = -H_1^{(2)}(x)$ ,  $dK_0(x)/dx = -K_1(x)$ ,  $dI_0(x)/dx = I_1(x)$ , etc., one obtains

$$\begin{aligned} a_1 H_0^{(1)}(h_0 r_1) + a_2 H_0^{(2)}(h_0 r_1) &= b_1 I_0(\kappa r_1) + b_2 K_0(\kappa r_1) \\ a_1 h_0 H_1^{(1)}(h_0 r_1) + a_2 h_0 H_1^{(2)}(h_0 r_1) &= -b_1 \kappa I_1(\kappa r_1) + b_2 \kappa K_1(\kappa r_1) \\ \eta H_0^{(1)}(h_0 r_2) &= b_1 I_0(\kappa r_2) + b_2 K_0(\kappa r_2) \\ \eta h_0 H_1^{(1)}(h_0 r_2) &= -b_1 \kappa I_1(\kappa r_2) + b_2 \kappa K_1(\kappa r_2) \end{aligned} \quad (20)$$

Using Equ. (20) one can shows that the transmission coefficient  $T$  is

$$T \equiv \eta / a_1 = \frac{pq}{a_{11}b_{11} + a_{12}b_{21}} \equiv |T| \exp[i\alpha(k)] \quad (21)$$

where

$$\begin{aligned} p &= h_0 [H_0^{(1)}(h_0 r_1) H_1^{(2)}(h_0 r_1) - H_0^{(2)}(h_0 r_1) H_1^{(1)}(h_0 r_1)] \\ q &= \kappa [I_0(\kappa r_2) K_1(\kappa r_2) + I_1(\kappa r_2) K_0(\kappa r_2)] \\ a_{11} &= h_0 H_1^{(2)}(h_0 r_1) I_0(\kappa r_1) + \kappa H_0^{(2)}(h_0 r_1) I_1(\kappa r_1) \\ a_{12} &= h_0 H_1^{(2)}(h_0 r_1) K_0(\kappa r_1) - \kappa H_0^{(2)}(h_0 r_1) K_1(\kappa r_1) \\ b_{11} &= \kappa K_1(\kappa r_2) H_0^{(1)}(h_0 r_2) - h_0 K_0(\kappa r_2) H_1^{(1)}(h_0 r_2) \\ b_{21} &= \kappa I_1(\kappa r_2) H_0^{(1)}(h_0 r_2) + h_0 I_0(\kappa r_2) H_1^{(1)}(h_0 r_2) \end{aligned} \quad (22)$$

Consider that analogous tunneling experiments with classical evanescent electromagnetic modes have shown the results are essentially in agreement with the quantum mechanical phase time approach [8] (note that the phase time has nothing to do with the phase velocity), we shall show the superluminal behaviors of modified Bessel beams via the phase time approach. To gain physics insight, we restrict ourselves to the extrapolated phase time approach [9-11] and, approximately, attribute

to the extrapolated phase time the physics meaning of the transit time for the modified Bessel beams propagating through the region between  $r = r_1$  and  $r = r_2$ . In our case, following the usual procedure, one can obtain the extrapolated phase time

$$\tau_T(r_1, r_2; k) = \left(\frac{d\omega}{dk}\right)^{-1} [r_2 - r_1 + \frac{d\alpha(k)}{dk}] \equiv \frac{r_2 - r_1}{v} \quad (23)$$

where  $d\omega/dk = c$  is the speed of light in vacuum, while  $v$  is related to the definition of the extrapolated phase time, and represents the group velocity of the modified Bessel beams propagating through the region between  $r = r_1$  and  $r = r_2$  (i.e. the group velocity of the modified Bessel beams tunneling through photonic potential barrier). Using Equ. (21), one has  $d\alpha(k)/dk = \text{Im}(d \ln T / dk)$ , where  $\text{Im}(X)$  represents the imaginary part of  $X$  and  $\ln T$  denotes the natural logarithm of  $T$ . Let  $w = r_2 - r_1$ , the group velocity, as the function of  $w$  and  $k$ , is

$$v(w, k) \equiv v = \frac{cw}{w + \text{Im}[d(\ln T) / dk]} \quad (24)$$

We show the superluminal behavior of the modified Bessel beams via numerical methods (by *Mathematica* 5.0), and give the diagrammatic curves related to the ratio  $v/c$  instead of the group velocity  $v$  itself. For simplicity we let  $L_0 \gg 1$  such that  $h_0 \approx k$ ,  $L_1 = \pi/10$ ,  $c = 1$ ,  $r_1 = 100$ , then  $r_2 = 100 + w$  and  $\kappa = \sqrt{400 - k^2}$  (see Equ. (17)).

Following Fig. 1-4 we summarize the superluminal behavior of the modified Bessel beams as follows:

- 1) The group velocity  $v$  of the modified Bessel beams is proportional to the width  $w = r_2 - r_1$ , which accords with the so-called Hartman effect [12];

2) For the wave number  $k$  satisfying  $0.6 \approx k_0 \leq k < 20$ , the group velocity  $v$  of the modified Bessel beams decreases as the wave number increases, which implies that the group velocity  $v$  increases as the height of photonic barrier increases;

3) For  $0.6 \approx k_0 \geq k > 0$ , the group velocity  $v$  rapidly increases as the wave number increases, which implies that the group velocity  $v$  increases as the height of photonic barrier decreases.

Of course, the numerical value of  $k_0$  depends on the choices of the parameters  $L_0$ ,  $L_1$  and  $w$ , etc. Furthermore, in the present case, according to the treatments of *Mathematica* 5.0, the points  $k = 0$  and  $k = 20$  are the singular points of  $v = v(k, w)$ . Therefore, as the wave number  $k$  approaches 0 or 20, the specific values of the group velocity  $v$  are meaningless, but this does not disturb what we concern. The programs by *Mathematica* 5.0 are given in Appendix A.

#### 4. Conclusions and prospects

We have shown that, in contrary to the ordinary Bessel beam of real argument, the modified Bessel beams have the superluminal behaviors. Furthermore, as a comparison between the superluminal behaviors of the modified Bessel beams and those of the evanescent plane-waves (the latter have been studied in photonic tunneling experiments), we also give the diagrammatic curves for the evanescent plane-waves that tunneling through a photonic barrier (the photonic barrier width is  $w = r_2 - r_1$ , and the photons within the photonic barrier satisfy  $\kappa = \sqrt{400 - k^2}$ ). As far as the superluminal behaviors of the modified Bessel beams and those of evanescent plane-waves are concerned, one can draw conclusions as follows:

(a) Their group velocities both increase with the increase of propagation distance (i.e., the width  $w = r_2 - r_1$ ), but in more detail, their curves of phase time vs propagation distance have some differences;

(b) For the wave number  $k$  satisfying  $0.6 \approx k_0 \leq k < 20$ , their curves of group velocities vs wave numbers are similar to each other;

(c) For the wave number  $k$  satisfying  $0.6 \approx k_0 \geq k > 0$ , their curves of group velocity vs wave number are different from each other. With the increase of wave number, the group velocities of the modified Bessel beams rapidly increase while those of the evanescent plane-waves fall off.

In our future work, we try to interpret the superluminal behaviors of the modified Bessel beams as mentioned above (c).

### **Acknowledgments**

The authors wish to acknowledge financial support from China National Natural Science Foundation 69971008 and the Excellent Young Teachers Program of MOE of China.

### **References:**

1. E. Recami, *Physica A* **252**, 586 (1998).
2. D. Mugnai, *Phys. Lett. A* **284**, 304 (2001).
3. W. A. Rodrigues, Jr., D. S. Thober, A. L. Xavier, Jr., *Phys. Lett. A* **284**, 217 (2001).
4. T. Sauter, F. Paschke, *Phys. Lett. A* **285**, 1–6 (2001).

5. M. Peshkin, Preprint, Physics/0006034.
6. N. P. Bigelow, C. R. Hagen, Phys. Rev. Lett. **87**, 059401 (2001).
7. J.T. Lunardi, Phys. Lett. A **291**, 66–72 (2001).
8. G. Nimtz, W. Heitmann, Prog. Quant. Electr. **21**, 81 (1997).
9. E. H. Hauge, J. A. Stoveneng, Rev. Mod. Phys. **61**, 917 (1989).
10. V. S. Olkhovsky, E. Recami, Phys. Reports **214**, 339 (1992).
11. R. Landauer, Th. Martin, Rev. Mod. Phys. **66**, 217 (1994).
12. Th. Hartman, J. Appl. Phys. **33**, 3427 (1962).

## Figure Captions

**Figure 1 (Color online):** The group velocity  $v$  as the function of the width  $w = r_2 - r_1$  (where  $k = 10$  and  $w = 0 \rightarrow 100$ ). This graph holds true for both the modified Bessel beams and the evanescent plane-waves.

**Figure 2 (Color online):** The phase time  $\tau$  as the function of the width  $w = r_2 - r_1$  (where  $k = 10$  and  $w = 0 \rightarrow 100$ ). The thick (and blue) curve corresponds to the modified Bessel beams; the thin (and red) curve corresponds to the evanescent plane-waves.

**Figure 3 (Color online):** The group velocity  $v$  as the function of the wave number  $k$  (where  $w = 10$  and  $k = 1 \rightarrow 19$ , or  $\kappa = \sqrt{400 - k^2} = 19.975 \rightarrow 6.245$ ). This graph holds true for both the modified Bessel beams and the evanescent plane-waves.

**Figure 4 (Color online):** The group velocity  $v$  as the function of the wave number  $k$  (where  $w = 10$  and  $k = 0.01 \rightarrow 5$ ). The thick (and blue) curve corresponds to the modified Bessel beams; the thin (and red) curve corresponds to the evanescent plane-waves.

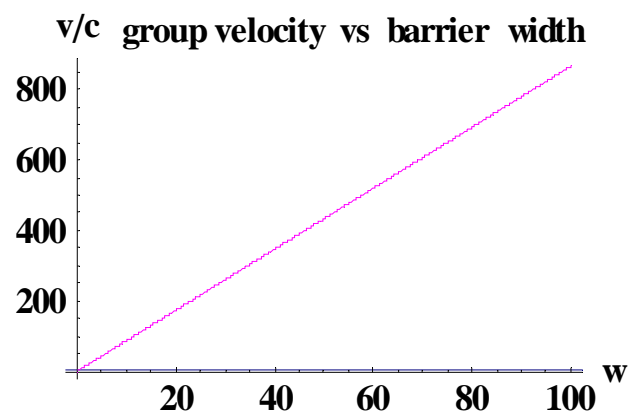


Figure 1

Wang *et al*, PRE

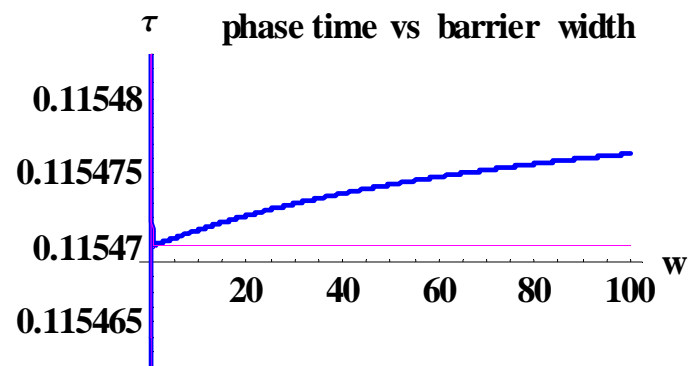


Figure 2

Wang *et al*, PRE

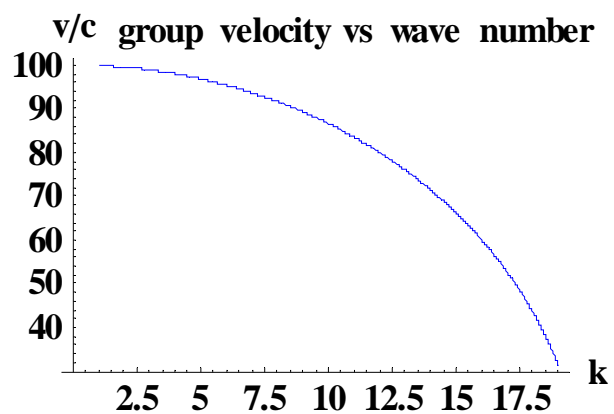


Figure 3

Wang *et al*, PRE

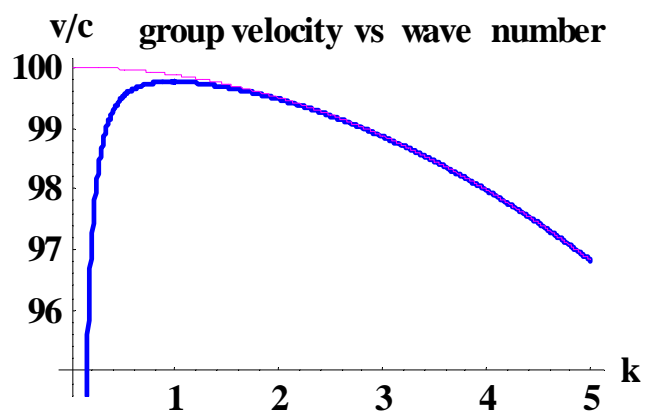


Figure 4

Wang *et al*, PRE

## Appendix A: Programs by *Mathematica* 5.0

### 1. Graph of phase time vs barrier width (for Fig. 2)

```

κ = √400 - k2
c = 1
r = 100 + w
H1[m_, x_] = BesselJ[m, x] + I * BesselY[m, x]
H2[m_, x_] = BesselJ[m, x] - I * BesselY[m, x]
BI[m_, x_] = BesselI[m, x]
BK[m_, x_] = BesselK[m, x]
p[k_, w_] = k * (H1[0, 100 k] * H2[1, 100 k] - H2[0, 100 k] * H1[1, 100 k])
q[k_, w_] = κ * (BI[0, κ * r] * BK[1, κ * r] + BI[1, κ * r] * BK[0, κ * r])
a11[k_, w_] = k * H2[1, 100 k] * BI[0, 100 κ] + κ * H2[0, 100 k] * BI[1, 100 κ]
a12[k_, w_] = k * H2[1, 100 k] * BK[0, 100 κ] - κ * H2[0, 100 k] * BK[1, 100 κ]
b11[k_, w_] = κ * BK[1, κ * r] * H1[0, k * r] - k * BK[0, κ * r] * H1[1, k * r]
b21[k_, w_] = κ * BI[1, κ * r] * H1[0, k * r] + k * BI[0, κ * r] * H1[1, k * r]
T[k_, w_] = 
$$\frac{p[k, w] * q[k, w]}{a11[k, w] * b11[k, w] + a12[k, w] * b21[k, w]}$$

α[k_, w_] = Log[T[k, w]]
f[k_, w_] = D[α[k, w], k]
τ[k_, w_] = 
$$\frac{w + \text{Im}[f[k, w]]}{c}$$

g1 = Plot[τ[10, w], {w, 0, 100}, TextStyle -> {FontSize -> 14,
    FontWeight -> "Bold", FontFamily -> "Times New Roman"}, 
    GridLines -> {None, {1}}, PlotPoints -> 1000, AxesOrigin -> {0, 0.115469},
    PlotStyle -> {Thickness[0.01], RGBColor[0, 0, 1]}, AxesLabel -> {"w", "τ"}, 
    PlotLabel -> "phase time vs barrier width"]
α1[k_, w_] = -ArcTan[
$$\left(\frac{\kappa^2 - k^2}{2k\kappa}\right) * \text{Tanh}[\kappa * w] - k * w$$

f1[k_, w_] = D[α1[k, w], k]
τ1[k_, w_] = 
$$\frac{w + f1[k, w]}{c}$$

g2 = Plot[τ1[10, w], {w, 0, 100}, TextStyle -> {FontSize -> 14,
    FontWeight -> "Bold", FontFamily -> "Times New Roman"}, 
    GridLines -> {None, {1}}, PlotPoints -> 1000, AxesOrigin -> {0, 0.115469},
    PlotStyle -> {Thickness[0.006], RGBColor[1, 0, 1]}, AxesLabel -> {"w", "τ"}, 
    PlotLabel -> "phase time vs barrier width"]
g3 = Show[g1, g2]

```

## 2. Graph of group velocity vs wave number (for Fig. 4)

```

 $\kappa = \sqrt{400 - k^2}$ 
c = 1
r = 100 + w
H1[m_, x_] = BesselJ[m, x] + I * BesselY[m, x]
H2[m_, x_] = BesselJ[m, x] - I * BesselY[m, x]
BI[m_, x_] = BesselI[m, x]
BK[m_, x_] = BesselK[m, x]
p[k_, w_] = k * (H1[0, 100k] * H2[1, 100k] - H2[0, 100k] * H1[1, 100k])
q[k_, w_] =  $\kappa * (BI[0, \kappa * r] * BK[1, \kappa * r] + BI[1, \kappa * r] * BK[0, \kappa * r])$ 
a11[k_, w_] = k * H2[1, 100k] * BI[0, 100\kappa] +  $\kappa * H2[0, 100k] * BI[1, 100\kappa]$ 
a12[k_, w_] = k * H2[1, 100k] * BK[0, 100\kappa] -  $\kappa * H2[0, 100k] * BK[1, 100\kappa]$ 
b11[k_, w_] =  $\kappa * BK[1, \kappa * r] * H1[0, \kappa * r] - k * BK[0, \kappa * r] * H1[1, \kappa * r]$ 
b21[k_, w_] =  $\kappa * BI[1, \kappa * r] * H1[0, \kappa * r] + k * BI[0, \kappa * r] * H1[1, \kappa * r]$ 
T[k_, w_] =  $\frac{p[k, w] * q[k, w]}{a11[k, w] * b11[k, w] + a12[k, w] * b21[k, w]}$ 
alpha[k_, w_] = Log[T[k, w]]
f[k_, w_] = D[alpha[k, w], k]
v[k_, w_] =  $\frac{c * w}{w + Im[f[k, w]]}$ 
g1 = Plot[v[k, 10], {k, 0.01, 5}, TextStyle -> {FontSize -> 14, FontWeight -> "Bold",
FontFamily -> "Times New Roman"}, GridLines -> {None, {1}}, PlotPoints -> 1000,
PlotStyle -> {Thickness[0.01], RGBColor[0, 0, 1]}, AxesLabel -> {"k", "v/c"}, PlotLabel -> "group velocity vs wave number"]
alpha1[k_, w_] = -ArcTan[ $\left(\frac{\kappa^2 - k^2}{2k\kappa}\right) * \text{Tanh}[\kappa * w]$ ] - k * w
f1[k_, w_] = D[alpha1[k, w], k]
v1[k_, w_] =  $\frac{c * w}{w + f1[k, w]}$ 
g2 = Plot[v1[k, 10], {k, 0.01, 5}, TextStyle -> {FontSize -> 14, FontWeight -> "Bold",
FontFamily -> "Times New Roman"}, GridLines -> {None, {1}}, PlotPoints -> 1000,
PlotStyle -> {Thickness[0.006], RGBColor[1, 0, 1]}, AxesLabel -> {"k", "v/c"}, PlotLabel -> "group velocity vs wave number"]
g3 = Show[g1, g2]

```